BIODEGRADABILITY AND BIOCOMPATIBILITY OF COPOLY(BUTYLENE SEBACATE-co-TEREPHTHALATE)S

Nina Heidarzadeh[1], Mehdi Rafizadeh[1*], Faramarz Afshar Taromi[1], Luís J. del Valle[2], Lourdes Franco[2], Jordi Puiggalí[2*]

[1]Department of Polymer Engineering and Color Technology, Amirkabir University of Technology, PO Box 15875-441, Tehran, IRAN
[2]Departament d'Enginyeria Química, Universitat Politècnica de Catalunya, Av. Diagonal 647, Barcelona E-08028, SPAIN

Correspondence to: **J. Puiggalí (E-mail: Jordi.Puiggali@upc.edu) and M. Rafizadeh (E-mail: mehdi@aut.ac.ir)**

ABSTRACT

In the present study poly(butylene sebacate-*co*-terephthalate)s having different compositions were synthesized with a high yield and a random distribution by thermal transesterification of poly (butylene sebacate) and poly (butylene terephthalate) homopolymers. The copolymer with the highest comonomer ratio was the least crystalline sample, although the melting peaks corresponding to both, sebacate-and terephthalate-rich phases were still observable in calorimetric heating runs. This copolymer was associated with interesting thermal and mechanical properties, as the maximum melting point was higher than 100 ºC and the storage modulus was also high (i.e. 1.1×10^9 N/m^2 and $1.7\ 10^8$ N/m^2 were determined just before and after the main glass transition temperature of -12 ºC).

As all studied samples were thermally stable up to temperatures clearly higher than the fusion temperature, they could be easily processed. Increasing the terephthalate content of the copolymers resulted in higher hydrophobicity, which had a minor influence on cell adhesion and proliferation of both fibroblast-like and epithelial-like cells. Hydrolytic and enzymatic degradability were assessed and the effect of composition and crystallinity on the degradation rate was investigated. Molecular weight measurements during exposure to a hydrolytic media indicated a first order kinetic mechanism during the initial stages of degradation before reaching a limiting molecular size, which was indicative of solubilization. The most amorphous sample appears as a highly promising biodegradable material ~~among the studied samples~~ since it ~~This sample not only~~ showed ~~the fastest~~ a significant weight loss during exposure to all selected degradation media, but also exhibited good performance and properties that were comparable to those characteristic of polyethylene.

Keywords: Poly(butylene terephthalate), poly(butylene sebacate), copolyesters, biocompatibility, hydrolytic degradation, enzymatic degradation.

INTRODUCTION

Development of bioplastics seems to be a promising strategy to solve environmental problems due to waste accumulation and even the depletion of fossil resources. Thereby, producing biodegradable polymers from renewable resources is currently among the main goals of the society. In fact, the production of bioplastics (i.e. biodegradable or bio-based materials) has been estimated to exceed 2 million tons by 2016 [1]. Despite the great deal of interests towards biodegradable polymers, it is rather difficult to find a material with all desired specifications for application as a commodity material (i.e. low cost, easy synthesis and processing, good thermal and mechanical properties, reasonable degradation rate under both hydrolytic and enzymatic media and even in some cases low cytotoxicity).

Polyesters can be generally considered as the main family of biodegradable polymers, a few of which show a good combination of properties. Polyglycolide, polylactide and poly (butylene succinate) (PBS) are the most common commercial homopolyesters. In fact, PBS is a biodegradable thermoplastic with thermal and mechanical properties closely comparable to those of the widely-used polyethylene and polypropylene [2-5].

It is well-known that biodegradability is influenced by multiple factors including surface wettability, crystallinity and chain flexibility [6]. Therefore, different strategies can be applied to control the degradation rate of a given polymer such as PBS. In this case, copolymerization, blending, formation of composites and even annealing processes have been considered [7-11].

Incorporation of aromatic units into an aliphatic polyester chain can greatly affect the mechanical properties while keeping the degradability. Recently aliphatic-aromatic polyesters have attracted a great deal of scientific attention. In particular poly butylene succinate-*co*-terephthalate) (PBST), poly ethylene succinate-*co*-terephthalate) (PEST) and poly(butylene

adipate-*co*-terephthalate) (PBAT) have been produced in an industrial scale, being also investigated by different academic/research groups. In fact, PBAT has been commercialized under the trademarks of Ecoflex, Origo-Bi (previously Eastar Bio), EndPol G, Skygreen SG300 and Fepol by BASF, Novamont (previously Eastman), Samsung, SK Chemicals and Far Eastern, respectively [12], and PBST has been commercialized as Green Ecopet by Teijin [12].

Studies concerning aliphatic-aromatic copolyesters based on longer dicarboxylic acid units are surprisingly scarce. Nevertheless, Jaisankar *et al.* [13, 14] reported the biodegradability of suberic and sebacic acid derivatives, with a lower degradation rate compared to that related to adipate derivatives. Differences were mainly attributed to the higher crystallinity of the sebacate copolymers.

The main goal of the present work was to prepare copolyesters based on 1,4-butanediol and sebacic and terephthalic acids so as to obtain materials with adequate thermal and mechanical properties as well as a good hydrolytic and enzymatic degradability. Furthermore, materials appear also interesting since 1,4 butanediol and sebacic acid can be obtained from bio-based feedstocks. Specifically, sebacic acid can be prepared by alkali fusion at high temperatures and alkali concentrations of ricinoleic acid. ~~Unfortunately,~~ Green synthesis of terephthalic acid has also been ~~is still not commercial despite its previously~~ reported. Therefore, production at a laboratory scale from isobutene or limonene, methyl coumalate, methyl pyruvate, furfural and *p*-cymene have been carried out [15-20]. In fact, production of a fully biobased polyethylene terephthalate from terephthalic acid derived from isobutene was launched in 2012 [21].

EXPERIMENTAL SECTION

Materials

Terephthalic acid (TA) was supplied by Shahid Toundgoyan Petrochemical Complex (Mahshar, Iran). 1,4-Butanediol (BDO) and sebacic acid (SeA), were bought from Daejung Chemical & Metal Co. Ltd. (Shiheung, Korea). Titanium tetrabutoxide (TBT) as polycondensation catalyst was purchased from Merck Co., (Darmstadt, Germany).

African green monkey kidney fibroblast-like (COS-7) and epithelial-like Madin-Darby Canine Kidney (MDCK) cells (ATCC, Manassas, VA, USA) were used in this work. Fetal bovine serum (FBS) was purchased from Gibco (Thermo Fisher Scientific Inc., Alcobendas, Spain). Lipases from porcine pancreas and *Pseudomonas cepacia* were purchased from Sigma-Aldrich (Barcelona, Spain).

Polymerization

The three selected copolymers (named as PBSeT with *x* denoting the molar ratio of sebacic acid units with respect to the total dicarboxylic content) were synthesized following a two-step melt polycondensation procedure based on a final transesterification between prepolymers of each dicarboxylic unit (i.e. terephthalic acid or sebacic acid) as shown in Figure 1.

a) Esterification of the selected dicarboxylic unit was carried out using an excess amount of BDO (i.e. 1.7:1 [OH]:[COOH]). The reaction mixture was first stirred for 30 min at 140 ºC and under a pressure of 3-3.5 bars. A flow of N_2 was provided to keep the required pressure while an electric condenser allowed separating the condensed water and the excess of diol. Reaction temperature was then increased to 200-215 ºC and 220 ºC, for sebacic and terephthalic acid derivatives, respectively. The reaction was stopped when no more water was recovered (approximately after 180 min). Reaction conversion was evaluated by weighting the recovered water at regular time intervals.

b) Transesterification between the appropriate mixtures of prepolymers (i.e. 0.3:0.7, 0.5:0.5 and 0.7:0.3 molar ratios between sebacate and terephthalate derivatives) was

carried out using TBT as catalyst (1.4 mmol for 1 mol of dicarboxylic acid). Firstly, reaction mixture was kept for 10 min at 200 ºC and 1.5-2 bars and finally temperature was increased up to 250 ºC while applying vacuum (20 mbar). The reaction was stopped when the mixer torque reached a maximum value (approximately after 150 min). Copolymers were dissolved in 1,1,1,3,3,3,-hexafluroisopropanol (HFIP), filtered and subsequently precipitated in water and finally washed several times with water, methanol and ether; and dried in a vacuum desiccator.

Measurements

Molecular weights were estimated using size exclusion chromatography (GPC) through a liquid chromatograph (Shimadzu, model LC-8A, Tokyo, Japan) equipped with an Empower computer program (Waters, Milford, MA USA). A PL HFIP gel column (Polymer Lab) and a refractive index detector (Shimadzu RID-10A, Tokyo, Japan)) were utilized. The polymer was dissolved and eluted in HFIP containing CF_3COONa (0.05 M) at a flow rate of 1 mL/min (injected volume of 100 µL, sample concentration of 2.0 mg/mL). The number and weight average molecular weights were calculated using polymethyl methacrylate standards.

Infrared absorption spectra were recorded in the 4000-600 cm^{-1} range with a Fourier Transform FTIR 4100 Jasco spectrometer (Tokyo, Japan) dotted with a Specac model MKII Golden Gate attenuated total reflection (ATR) cell.

^{1}H-NMR spectra were acquired via a Bruker AMX-300 spectrometer (Bremen, Germany) operating at 300.1 MHz. Chemical shifts were calibrated using tetramethylsilane as an internal standard. A mixture (1:1 *v*/*v*) of deuterated chloroform and trifluoroacetic acid was used as the solvent.

Calorimetric data were obtained by differential scanning calorimetry with a TA Instruments Q100 series (New Castle, DE, USA) with T_{zero} technology and equipped with a

refrigerated cooling system (RCS). Experiments were conducted under a flow of dry nitrogen with a sample weight of approximately 5 mg and calibration was performed with indium. A first heating run (20 ºC/min) was performed to determine melting temperature and enthalpy, whereas a cooling run (10 ºC/min) was carried out after keeping the sample in the melt state for 3 minutes to erase the thermal history and to obtain crystallization data. Finally, a second heating run (20 ºC/min) was performed to characterize the melt crystallized sample.

Thermal degradation was studied at a heating rate of 10 ºC/min with around 5 mg samples in a Q50 thermogravimetric analyzer (TGA) of TA Instruments (New Castle, DE, USA) and under a flow of dry nitrogen. Test temperatures ranged from 50 to 600 ºC.

A TA Instruments DMA Q800 (New Castle, DE, USA) was used to study the dynamic-mechanical properties of the materials. Prismatic rectangular samples (ca $10 \times 12 \times 1.3$ mm^3) were analyzed in single-cantilever mode at 1 Hz and 10 µm strain amplitude at 3 °C/min from -100 to 100 °C.

X-ray diffraction patterns were acquired using a Bruker D8 Advance model (Bruker, Karlsruhe, Germany) with Cu Kalpha radiation (lambda = 0.1542 nm) and the geometry of Bragg–Brentano, theta–2theta. A one-dimensional Lynx Eye detector (Bruker, Karlsruhe, Germany) was employed. Deconvolution of diffraction peaks was performed with the Peak Fit v4 program by Jandel Scientific Software (San Rafael, CA, USA).

Contact angles (CA) were measured at room temperature via sessile drops using an OCA-15 plus Contact Angle Microscope (Dataphysics Instruments GmbH, Filderstadcity, Germany) and SCA20 software. Contact angle values of the right and left sides of distilled water and fetal bovine serum (FBS) drops were measured and averaged. Measurements were performed 10 s after the drop (0.5 µL) was deposited on the sample surface. All CA data were obtained by average of six measurements on different surface locations.

Degradation studies

Thermally molded films were employed for different degradation studies. Polymers were heated at 10 ºC above their melting point for 2 min by means of a hydraulic press equipped with heating plates and a temperature controller (Graseby Specac, Kent, England). Pressure was progressively increased to 3-4 bars. Polymer films with a thickness of approximately 150 µm were recovered after cooling the mold to room temperature and subsequently cut to the desired size.

In vitro hydrolytic degradation assays were carried out in a pH 7.4 phosphate buffer (19.268 g of $Na_2HPO_4.12H_2O$ and 1.796 g of KH_2PO_4 in 1L of deionized water) at 37 ºC and under the accelerated conditions provided by raising temperature to 70 ºC. Samples (2×2 cm^2 square pieces) were kept under orbital shaking in bottles filled with 20 mL of the degradation medium and sodium azide (0.03 wt-%) to prevent microbial growth for the selected exposure times. The samples were then thoroughly rinsed with distilled water, dried to constant weight under vacuum and stored over P_4O_{10} before analysis. Degradation studies were performed in triplicate and the given data were reported according to the average values.

The enzymatic studies were carried out with lipases from porcine pancreas (30–90 U/mg) and *Pseudomonas cepacia* (≥ 40 U/mg) using 3 replicates. All samples (1×1 cm^2 square pieces) were exposed to 2 mL of phosphate buffer (pH 7.4) containing the enzyme (100 mg/L) along with sodium azide (0.03% w/v) and calcium chloride (5 mM). Solutions were renewed every week to prevent enzymatic activity loss. Samples were extracted, washed and dried as previously described.

Scanning electron microscopy (SEM) was employed to examine the morphology of films after different times of exposure to the selected degradation media. Carbon coating was accomplished with a Mitec k950 Sputter Coater (fitted with a film thickness monitor k150x) (Quorum Technologies Ltd., West Sussex, UK). SEM micrographs were obtained

SEM micrographs were obtained with a Focus Ion Beam Zeiss Neon 40 instrument (Carl Zeiss, Oberkochen, Germany).

Weight retention (W_r) of the specimens was determined by the percentage ratio of weight after degradation (W_d) to the initial weight before degradation (W_0):

$$W_r = W_d / W_0 \times 100 \quad (1)$$

Cell adhesion and proliferation assays

COS-7 and MDCK cells were cultured in Dulbecco's modified Eagle medium (DMEM) as previously reported [22].

Square pieces ($10 \times 10 \times 0.15$ mm^3) of hot-pressed films were placed and fixed in each well of a 24-well culture plate with a small drop of silicone (Silbione® MED ADH 4300 RTV, Bluestar Silicones France SAS, Lyon, France). They were then sterilized by UV-radiation in a laminar flux cabinet for 15 min. The samples were stabilized for 24 h in 1 mL of medium under culture conditions. For the cell adhesion and proliferation assays, aliquots of 50–100 µL containing 5×10^4 and 2×10^4 cells, respectively, were seeded onto the films in each well containing 1 mL of medium and incubated for 24 h (adhesion assay) or 7 days (proliferation assay).

Samples were evaluated by the standard adhesion and proliferation methods based on a simple modification of the ISO10993-5:2009 standard test that describes the appropriate methodology to assess the *in vitro* cytotoxicity of the medical devices. Finally, the cellular viability on materials was evaluated through the MTT method [22]. This colorimetric assay was evaluated by means of a microplate reader (EZ Read 400 Research, Biochrom, Cambridge, UK).The study was carried out using five replicates and the results were averaged. Samples with adhered and grown cells on the mats were fixed with

2.5% *w/v* formaldehyde at 4 °C overnight. They were subsequently dehydrated and processed for observation by scanning electron microscopy.

Statistical analysis

Values were averaged and graphically represented, together with their respective standard deviations. Statistical analysis was performed by one-way ANOVA test to compare the means of all groups, and then the test of Tukey was applied to determine a statistically significant difference between two groups. The test confidence level was set at 95% ($p<0.05$) (Origin Pro V8 software, OriginLab Corp., MA, USA)

RESULTS AND DISCUSSION

Synthesis and characterization of PBSeT-*x* copolymers

Copolymers were synthesized with a high yield (i.e. close to 90%), had molecular weights independent of the composition and typical polydispersity indices for polycondensation processes (i.e. > 2) as summarized in Table 1. Infrared spectra showed typical bands of aliphatic (2930 and 2850 cm^{-1}), C=O (1712 cm^{-1}), aromatic C-O (1283 and 1179 cm^{-1}, asymmetric and symmetric stretching, respectively), aliphatic C-O (1220 and 1079 cm^{-1}, asymmetric and symmetric stretching, respectively) and aromatic (729 cm^{-1}) groups (Figure 2), attributing the main differences to the relative intensity of the aliphatic (inset of Figure 2) or the aromatic bands.

Determination of copolymer composition and microstructure (Table 2) was performed by means of ^{1}H NMR spectra as the characteristic signals of each unit and the sequence type could be determined as shown in Figure 3 for PBSeT-70. Signal at 8.15 ppm (protons of terephthalate units, T) and 2.43 ppm ($COCH_2$ protons of sebacate units, Se) were used to determine the corresponding f_T and f_{Se} mole fractions.

The OCH_2 butanediol protons were highly sensitive to the neighbouring dicarboxylic acid units and consequently 4 triplets were detected for all studied samples. The respective areas of such peaks were used to determine the fractions corresponding to TBT (f_{TT}), TBSe (f_{TSe}), SeBT (f_{SeT}), and SeBSe (f_{SeSe}) sequences. These values allowed calculating the probability of finding a T unit next to a SeB sequence (P_{SeT}) as well as the probability of finding a sebacate unit next to a TB sequence (P_{TSe}):

$$P_{SeT} = f_{SeT} / f_{Se} \quad (1)$$

$$P_{TSe} = f_{TSe} / f_{Se} \quad (2)$$

Finally, block length of SeB and TB sequences were calculated as:

$$L_{nSeB} = 1 / P_{SeT} \quad (3)$$

$$L_{nTB} = 1 / P_{TSe} \quad (4)$$

The degree of randomness (r) can be evaluated as the addition of the two probabilities (P_{SeT} and P_{TSe}), being values of 2, 1 and <1 characteristic of alternating, random, and blocky distributions. The limit value of 0 corresponds to a mixture of the two homopolymers. Values summarized in Table 2 indicate a composition close to the theoretical one and a degree of randomness close to 1.0 which demonstrate the effectiveness of the transesterification process.

Thermal and mechanical properties of PBSeT-*x* copolyesters

Copolyesters showed a complex melting behaviour since peaks associated to both sebacate and terephthalate crystalline phases could be observed at 42-47 ºC and 89-163 ºC, respectively (Figure 4). Melting point of the terephthalate phase clearly decreased with increasing the comonomer content as an evidence of the entrapment of foreign units. It should be pointed out that a complete fusion required a relatively high temperature and specifically the most amorphous sample of PBSeT-50 melted at a temperature higher than 100 ºC.

Crystallinities of samples were determined based on experimental melting enthalpy for 100% crystalline PBT (142 J/g) [23] and a value of 211 J/g for 100% crystalline PBSe, which was estimated from the group contribution theory [24]. In this way, crystallinities for each phase along with the global crystallinity were estimated as summarized in Table 3. Logically, the total melting enthalpy and the estimated crystallinity both decreased with the comonomer content, and were minima for the intermediate composition (i.e. PBSeT-50). Therefore, crystallinity decreased to 10% which was significantly lower than those determined for PBSeT-30 (24%) and PBSeT-70 (19%) samples.

All samples were also able to crystallize from the melt as summarized in Table 3 despite the random distribution of terephthalate and sebacate units. Crystallinities were even slightly higher than those determined from solution precipitated samples.

The predominant amorphous phase was characterized by a single glass transition temperature that ranged between -28 ºC and -39 ºC and increased with increasing the terephthalate content. This amorphous phase was constituted by the random sequences including both terephthalate and sebacate units and appeared at intermediate temperatures of those reported for PBT (66 ºC [25,26]) and PBSe (-59 ºC [27]). Glass transitions corresponding to terephthalate- and sebacate- rich phases were not detected in DSC scans since the more regular sequences are expected to be incorporated in the corresponding crystalline phases. Indeed, the complex DSC pattern made it difficult to observe T_gs close to the typical value of PBT.

Glass transition temperatures were better determined by DMTA as shown in Figure 5 where a wide dissipation band in the tan δ function and a steeped decrease in the storage modulus, E', were detected. All samples showed a predominant loss tangent peak in the narrow temperature range between -14.3 ºC and -5.3 ºC. This temperature increased with the aromatic content but the variation was not so great as could be expected taking into account the

reported glass transition temperatures for homopolymers, the copolymer composition and the typical Fox equation (i.e. $1/T_g = w_1/T_{g1} + w_2/T_{g2}$ where w_i and T_{g1} represent the weight fraction and the glass transition temperature of each component and homopolymer, respectively) [28]. Specifically, theoretical values should range between -35 ºC and 3.1 ºC, which involves a clearly wider temperature range. The significant discrepancy between experimental (i.e. -14.3 ºC) and theoretical (i.e. -35 ºC) values for PBSeT-70 suggests that the amorphous phase has become impoverished of sebacate units. This feature is in agreement with the observed incorporation of them in the terephthalate-rich crystal phase and also by the presence of another amorphous phase rich on sebacate units. Thus, a low temperature relaxation peak was detected around -78 ºC (i.e. slightly lower than the expected value for PBSeT [27]). In contrast, only a small peak around 60 ºC was observed (see inset of Figure 5) in the terephthalate-rich PBSeT-30 copolymer.

The storage modulus of all samples was high before the first glass transition temperature and increased from 0.9×10^9 N/m^2 to 2.1×10^9 N/m^2 when f_T increased from 0.31 to 0.65. Table 4 also shows the dependence of modulus on temperature and reveals that it maintains a relatively high value at room temperature (i.e. after the main relaxation peak) since moduli between 4.1×10^8 N/m^2 and 2.6×10^8 N/m^2 were determined as shown in Table 5. Modulus after the main glass transition temperature was more influenced by crystallinity than by composition and therefore PBSeT-50 had a lower modulus compared to PBSeT-70. In any case, the most amorphous sample still exhibited a high mechanical performance around 100 ºC, with a modulus in 10^8 N/m^{2}range.

All copolymers were thermally stable up to an onset degradation temperature higher than 320 ºC (Table 5) and obviously than the corresponding melting point. Thermal decomposition proceeded according to two steps (Figure 6), with the first one occurring at a temperature close to that reported for PBT [29] and being clearly the predominant process (92-97%). The

temperature of the DTGA peak slightly increased with increasing the sebacate content as well as the intensity of the DTGA peak associated with the second decomposition step. Practically, no differences were found between the char yields although the greatest value was determined for the sample with the highest aromatic content (i.e. 5.2% with respect to 2.6%-3.3 %).

Biocompatibility of PBSeT-*x* copolymers

Characteristics of polymer surfaces may have some influences on the attachment and growth of cells. Figure 7a shows that copolymer film surfaces were slightly hydrophilic since in all cases, contact angles of water droplets were lower than 90º. A small variation (i.e. from 83º to 74º) was detected when the aromatic content decreased and consequently the surface of PBSeT-70 was expected to be more favourable for cell colonization as has been reported for other systems [30]. The increase of hydrophilicity could also influence the degradability of the sample but as it will then be discussed, the main and most decisive influencing factor could be attributed to the greater susceptibility of the aliphatic ester bonds to hydrolysis. Results obtained using FBS drops (Figure 7b) were clearer since the dependence with the sebacate content was higher (i.e. contanct angles of 62º, 68º and 74º were determined for PBSeT-70, PBSeT-50 and PBSeT-30, respectively).

Biocompatibility of the different copolymers was evaluated through adhesion and proliferation assays using both epithelial-like and fibroblast-like cell lines (MDCK and COS-7 cells, respectively). In general, epithelial cells tend to form a monolayer of flat cells with a polygonal/irregular shape as shown in Figure 8. These cells require a great surface to be adhered through their basal domains and consequently are expected to be more sensitive to adverse surfaces than fibroblast-like cells. Morphologies depicted in Figure 8 revealed the formation of clusters of epithelial cells over the surfaces of the three studied copolymers. Cells tended towards a flat shape with their base fully extended on the copolymer film

surfaces and formed lamellipodia (see arrows) that emerged from the cytoplasmic extensions. A widespread adherence to the polymer surface was achieved by multiple tiny hairs (<1 μm) that emerged from the cell membranes.

Quantitative results indicated that the adhesion viability of COS-7 cells was satisfactory for all samples (in 89%-92% range), while a slight decrease was detected for the long time proliferation event (84%-87% range) (Figure 8d). Better results were attained for the more hydrophilic sebacate-rich sample since minimum differences between adhesion and proliferation assays were observed (89% and 87%). In any case, differences could not be considered statistically significant.

A slightly worse adhesion viability of epithelial-like MDCK cells (83%-85%) was found (Figure 8e), demonstrating the higher susceptibility of these cells to the surface characteristics. However, cell viability increased in the long-term event (90%-93%), indicating the capability of these cells to overcome the initial adverse effect and the biocompatibility of all studied copolymers. In summary, viability was slightly influenced by cell morphology and probably by the presence of some terminal groups that could cause a lower adhesion for the epithelial-like cells. No cytotoxic effects due to degradation products could be detected in the proliferation assays performed with MDCK cells.

Hydrolytic degradation

Copolyesters were hydrolytically degradable under accelerated condition provided by increasing the temperature up to 70 ºC as shown in Figures 9a and 9b. Thus, weight loss regularly increased during exposure and reached values between 30% and 52% after 60 days. Finally, after 300 days of exposure, the weight loss was severe for PBSeT-70 and PBSeT-50 with values of 88% and 78%, respectively. However, PBSeT-30 showed a residual weight of 50%. Thus, the degradation of these PBSeT copolymers was clearly increased

with the increased content of sebacic acid units (Figure 9b). In contrast, a weight loss lower than 5% and 10% was determined after 60 and 300 days of degradation at 37 ºC (Figure 9a), being difficult to establish a clear differences between the different studied samples.

^{1}H NMR spectra of samples exposed to the hydrolytic medium at 70 ºC (Figure 9c) clearly indicated that degradation mainly proceeded through the cleavage of ester groups involving sebacate units. Specifically, the relative intensity of the peak corresponding to the SeBSe sequence clearly diminished after 60 days of exposure and practically disappeared after 300 days. Note that this feature was clearly observed for the sebacate rich sample (PBSeT-70). Relative intensities of TBSe and SeBT peaks also decreased during degradation as expected from the preferred degradation of aliphatic ester linkages. In the same sense the TBT became clearly predominant in the residual product. NMR spectra showed also the appearance of well-defined triplets around 4.00 ppm that should be attributed to -CH_2OH terminal groups. It is also remarkable that only slight differences were found between PBSeT-70 and PBSeT-50 samples despite the significantly different aliphatic content. Logically, degradation was lower for PBSeT-50 (i.e. weight losses of 78% with respect to 88% were found after 300 days of exposure). This small difference suggests that degradation became slightly hindered when SeBSe sequences were arranged into crystalline and less accessible domains as it is the case of PBSeT-70.

Clear differences on the degradability have been found depending on the composition, being PBSeT-70 the most degradable sample. Figure 11 show the WAXD profiles of PBSeT copolymers from the films degraded for 60 and 300 days. The crystallized PBSeT-30 has the Bragg peaks at values of the scattering vector ($q = 2\pi/d$) of 6.708, 11.490, 12.326, 14.610, 16.576, 17.758, 20.653 and 22.117 nm-1. Two amorphous halos at q = 14.321 and 20.896 nm-1 are required to reproduce the observed WAXD intensity. This WAXD profiles of PBSeT-30 was similar to the WAXD profiles in the heating process of PBT

crystallized at 188.2 ºC and it correspond to the alpha-form. However, the increase of sebacic acid units to 50% and 70% change the WAXD profiles with two Bragg peaks with high intensity at q = 14.875 and 17.260 nm-1 for PBSeT-50, and q = 14.813 and 17.114 nm-1 for PBSeT-70.

However, the WAXD profiles changed during the degradation for 60 and 300 days; and finally, the WAXD profiles were similars at the end of the degradation on the 300 days. In this sense, the crystallinity of PBSeT samples were calculated as about 50% for initial samples, and as 60% and 70% at 60 and 300 days of hydrolitic degradation using a mode accelerated at 70 ºC (Figure 10). ~~Crystallinity plays a determinant role such that the more amorphous PBSeT-50 sample shows the highest degradability despite having an intermediate composition. Results concerning the copolymers richer on terephthalate and sebacate units were somehow contradictory and reflected the inaccuracies that could be committed when only weight loss measurements were considered. In this way, as opposed to data obtained from NMR spectra, PBSeT-30 seems to be more degradable than PBSeT-70 (i.e. the weight lost levels after 60 days of exposure were 31% and 16%, respectively) (Figure 9b). Such discrepancy may be due to the different solubility of the degradation fragments.~~

Molecular weight measurements of samples exposed to the hydrolytic medium showed a quick degradation process since only seven days were required for a decrease more than 50% of the initial number and weight average molecular weights. In this case, the slowest decrease was observed for the PBSeT-30 sample, in agreement with the expected behaviour ~~contradicting again the conclusions from remaining weight measurements~~. A similar rate for the molecular weight decrease was detected for PBSeT-50 and PBSeT-70 samples, suggesting that chain breakages could take place in the lamellar folding surface causing a decrease in the molecular weight but not a remarkable change in the remaining weight since crystal entities were practically insoluble.

It is assumed that hydrolytic degradation of polyesters in the early stages can be simulated according to a first order mechanism that lead to an exposure time dependence of molecular weight given by equation 5 [31,32]:

$$M = M_0 \, e^{-kt} \qquad (5)$$

where M is the molecular weight at time t, M_0 is the initial molecular weight and k the kinetic constant.

Figure 11 shows a good fit between experimental and simulated data when the exposure time was low and a considerable deviation at times higher than 7 days. It is clear that molecular weight tended to asymptotic values that should be related with the molecular size required to get soluble fragments. Consequently, the first order approximation did not make sense at higher exposure times. Values of kinetic constants allowed quantifying the degradation rates and showed clear differences between PBSeT-30 and the other two copolymers (i.e. 0.18 $days^{-1}$ in front of 0.34-0.40 $days^{-1}$ from number average data and 0.20 $days^{-1}$ in front of 0.27-0.30 $days^{-1}$ from weight average data).

SEM micrographs (Figure 12) clearly showed a degradation process that started through the formation of cracks on the film surface and the subsequent development of deep craters as a result of the hydrolysis of the inner material and the release of degradation products. Surfaces of exposed materials were clearly different from both the smooth texture of the initial samples as detected at low magnification and the slightly granular texture observed at high magnification. Although the initial texture of the three copolyesters was similar, clear differences could be observed between them after exposure to the hydrolytic medium for 60 days. Thus, the surface of PBSeT-30 after degradation was characterized by the presence of a limited number of holes with a reduced size while abundant, large sized and depth holes were developed in the surface of both, PBSeT-50 and PBSeT-70 samples. It is also worth noting

that at high magnifications the surface of these materials became rough due to the formation of multiple striations.

Enzymatic degradation

Copolyesters were also susceptible to the enzymatic attack of lipases as shown in Figure 13. The degradation rate was moderate but progressed steadily over the exposure time, resulted in weight losses between 8% and 16% after 60 days of exposure to a porcine lipase medium and between 14% and 25% after exposure for the same period to a *Pseudomonas cepacia* lipase medium.

The nature of the lipase had therefore an influence on degradability, suggesting a different fitting of the active sites of the enzyme with the polymer chains. Nevertheless, the trends observed using the more aggressive enzymatic medium (*Pseudomonas cepacia*) indicated a higher degradation for PBSeT-50 and lower degradation for PBSeT-30 and PBSeT-70. The degradability is enhanced by the high amorphous content as it is well-known that the enzymatic attack hardly occurs in closely-packed crystalline regions. Por ello, todas las muestras estudiadas con una cristalinidad inicial muy similar (cercana al 50%) deberían mostrar la misma degradación enzimática. Por otro lado,

~~were similar to those found for the hydrolytic degradation which resulted in higher and lower degradation rates for PBSeT-50 and PBSeT-30 samples, respectively. In the first case, degradability was enhanced by the high amorphous content as it is well-known that the enzymatic attack hardly occurs in closely-packed crystalline regions. In the second case~~, the slow degradation of the terephthalate-rich copolymer arises from the lower specificity of selected enzymes towards aromatic polyester substrates, the high crystallinity and the high

stiffness of the aromatic rich chains which hinders the location of ester groups in the active sites of the selected enzyme [33].

Morphological observations (Figure 12) of the film surfaces of samples exposed to enzymatic media demonstrated again the formation of craters and holes in an extension that was consistent with the weight loss measurements. In addition, surface roughness was clearly observed even at low magnification for the most degradable PBSeT-50 samples.

CONCLUSIONS

Thermal transesterification reactions between poly (butylene sebacate) and poly (butylene terephthalate) led to copolyesters with a random monomer distribution. These copolyesters were not cytotoxic as demonstrated by adhesion and proliferation of epithelial-like and fibroblast-like cell lines. The obtained aromatic-aliphatic copolyesters were thermally stable up to 320 ºC, and no significant differences were observed between samples with different composition.

The copolymer constituted by a similar ratio of sebacate and terephthalate units (PBSeT-50) had the highest amorphous content. Nevertheless, crystalline domains with melting temperatures above 100 ºC were detected when samples were precipitated from solution or were slowly cooled from the melt state. The aromatic content together with the relatively high melting temperature led to materials with good mechanical properties and specifically with storage modulus values around 10^8 N/m^2 at temperatures close to the fusion.

Samples were both hydrolytically and enzymatically degradable, with a higher degradation rate for PBSeT-50 as a clear evidence of a predominant influence of crystallinity on degradability. In summary, PBSeT-50 appears to be a very interesting biocompatible material due to its high degradability and its mechanical and thermal properties comparable to those exhibited by polyethylene.

Acknowledgements. Authors are in debt to supports from MINECO and FEDER (MAT2015-69547-R), the Generalitat de Catalunya (2014SGR188).

REFERENCES

[1] <http://www.european-bioplastics.org/>, 2014.

[2] Fujimaki T. Processability and properties of aliphatic polyesters,'BIONOLLE', synthesized by polycondensation reaction, Polym Degrad Stab 1998;59(1):209-214. doi:10.1016/S0141-3910(97)00220-6

[3] Ahn B, Kim S, Kim Y, Yang J, Synthesis and characterization of the biodegradable copolymers from succinic acid and adipic acid with 1, 4-butanediol, J Appl Polym Sci 2001;82(11):2808-2826. doi: 10.1002/app.2135

[4] Nikolic MS, Djonlagic J, Synthesis and characterization of biodegradable poly (butylene succinate-co-butylene adipate) s, Polym Degrad Stab 2001;74(2):263-270. doi.org/10.1016/S0141-3910(01)00156-2

[5] E. Yoo, S. Im, Melting behavior of poly (butylene succinate) during heating scan by DSC, J Polym Sci Part B Polym Phys 1999;37(13):1357-1366. doi:10.1002/(SICI)1099-0488(19990701)37:13<1357::AID-POLB2>3.0.CO;2-Q

[6] Díaz A, Katsarava R, Puiggalí J, Synthesis, properties and applications of biodegradable polymers derived from diols and dicarboxylic acids: From polyesters to poly (ester amide) s, Int j mol sci 2014;15(5):7064-7123. doi: 10.3390/ijms15057064

[7] Tachibana Y, Giang NTT, Ninomiya F, Funabashi M, Kunioka M, Cellulose acetate butyrate as multifunctional additive for poly (butylene succinate) by melt blending: Mechanical properties, biomass carbon ratio, and control of biodegradability, Polym Degrad Stab 2010;95(8):1406-1413. doi: 10.1016/j.polymdegradstab.2010.01.006

[8] Cho K, Lee J, Kwon K, Hydrolytic degradation behavior of poly (butylene succinate) s with different crystalline morphologies, J appl polym sci 2001;79(6):1025-1033. doi: 10.1002/1097-4628(20010207)79:6<1025::AID-APP50>3.0.CO;2-7

[9] Jin HJ, Lee BY, Kim MN, Yoon JS, Thermal and mechanical properties of mandelic acid-copolymerized poly (butylene succinate) and poly (ethylene adipate), J Polym Sci Part B Polym Phys 2000;38(11):1504-1511. doi: 10.1002/(SICI)1099-0488(20000601)38:11<1504::AID-POLB100>3.0.CO;2-4

[10] Okamoto K, Sinha Ray S, Okamoto M, New poly (butylene succinate)/layered silicate nanocomposites. II. Effect of organically modified layered silicates on structure, properties, melt rheology, and biodegradability, J Polym Sci Part B Polym Phys 2003;41(24):3160-3172. doi: 10.1002/polb.10708View

[11] Tserki V, Matzinos P, Pavlidou E, Vachliotis D, Panayiotou C, Biodegradable aliphatic polyesters. Part I. Properties and biodegradation of poly (butylene succinate-co-butylene adipate), Polym degrad stab 2006;91(2):367-376. doi:10.1016/j.polymdegradstab.2005.04.035

[12] Niaounakis M, editor. Biopolymers Reuse, Recycling, and Disposal, Chap. 1: Introduction to Biopolymers, William Andrew Publishing, Elsevier, 2013. pp. 1-75. doi:10.1016/B978-1-4557-3145-9.00001-4

[13] Jaisankar V, Nanthini R, Ravi A, Karunanidhi M, A study on biodegradation of aliphatic-aromatic random copolyesters, J Polym Mater 2009;26(2):157-166.

[14] Jaisankar V, Nanthini R, Karunanidhi M, Ravi A, Study on biodegradable random copolyesters derived from 1, 4-butanediol, terephthalic acid and adipic acid/sebacic acid, Asian J Chem 2010;22(7):5077.

[15] Peters MW, Taylor JD, Jenni M, Manzer LE, Henton DE, Integrated process to selectively convert renewable isobutanol to p-xylene, US Patent 20,110,087,000;2011.

[16] Berti C, Binassi E, Colonna M, Fiorini M, Kannan G, Karanam S, Mazzacurati M, Odeh I, Bio-Based terephthalate polyesters, US Patent 20,100,168,461;2010.

[17] Jacquel N, Saint-Loup R, Pascault J-P, Rousseau A, Fenouillot F, Bio-based alternatives in the synthesis of aliphatic–aromatic polyesters dedicated to biodegradable film applications, Polymer 2015;59:234-242. doi:10.1016/j.polymer.2014.12.021

[18] Lee JJ, Kraus GA, One-pot formal synthesis of biorenewable terephthalic acid from methyl coumalate and methyl pyruvate. Green Chem 2014;16:2111-2116. doi: 10.1039/C3GC42487A

[19] Tachinaba Y, Kimura S, Kasuya K-I, Synthesis and Verification of Biobased Terephthalic Acid from Furfural. Sci Rep 2015;5:8249. doi: 10.1038/srep08249

[20] Colonna M, Berti C, Fiorini M, Binassi E, Mazzacurati M, Vannini M, Karanam S. Synthesis and radiocarbon evidence of terephthalate polyesters completely prepared from renewable resources. Green Chem 2011;13:2543–2549. doi: 10.1039/C1GC15400A.

[21] Toray Industries, Inc (2012) Toray and Gevo Sign Bio-Paraxylene Offtake Agreement for the World's 1st Pilot-scale Fully Renewable, Bio-based Polyethylene Terephthalate (PET) Production. Available at http://www.toray.com/news/rd/nr120627.html.

[22] Llorens E, Del Valle LJ, Díaz A, Casas MT, Puiggalí J, Polylactide nanofibers loaded with vitamin B6 and polyphenols as bioactive platform for tissue engineering, Macromol Res 2013;21(7):775-787. doi:10.1007/s13233-013-1090-x

[23] Illers K-H, Heat of fusion and specific volume of poly (ethylene terephthalate) and poly (butylene terephthalate, Colloid Polym Sci 1980;258(2):117-124. doi:10.1007/BF01498267

[24] Van Krevelen DW, Calorimetric properties (Chapter 5), In Properties of Polymers (Third edition). Amsterdam:Elsevier, 1997. p. 109-127. doi:10.1016/B978-0-444-82877-4.50012-3

[25] Heidarzadeh N, Rafizadeh M, Taromi FA, Bouhendi H, Preparation of poly (butylene terephthalate)/modified organoclay nanocomposite via in-situ polymerization: Characterization, thermal properties and flame retardancy, High Perform Polym 2012;24(7):589-602. doi:10.1177/0954008312446646

[26] <http://www.polymerprocessing.com/polymers/PBT.html>, 2000.

[27] <http://polymerdatabase.com/polymer/physics/Polymer%20Tg.htm>, 2015.

[28] Fox TG, Influence of diluent and of copolymer composition on the glass temperature of a polymer system, Bull Am Phys Soc 1956;1(2):123-35.

[29] Chrissafis K, Paraskevopoulos K, Bikiaris D, Thermal degradation mechanism of poly (ethylene succinate) and poly (butylene succinate): comparative study, Thermochim Acta 2005;435(2):142-150. doi:10.1016/j.tca.2005.05.011

[30] Llorens E, Del Valle LJ, Ferrán R, Rodríguez-Galán A, Puiggalí J, Scaffolds with tuneable hydrophilicity from electrospun microfibers of polylactide and poly (ethylene glycol) mixtures: morphology, drug release behavior, and biocompatibility, J Polym Res 2014;21(2):1-15. doi:10.1007/s10965-014-0360-4

[31] Anderson J, Hollinger J, Perspectives on the in vivo responses of biodegradable polymers, In: Hollinger JO, editor. Biomedical Applications of Synthetic Biodegradable Polymers. Boca Raton, CRC Press, 1995. P. 223.

[32] Li S, Vert M, Biodegradation of aliphatic polyesters, In: Scott G, Gilead D, editors. Degradable Polymers: Principles and applications. Dordrecht, Springer Netherlands, 1995. p. 43-87.

[33] Nagata M, Kiyotsukuri T, Ibuki H, Tsutsumi N, Sakai W, Synthesis and enzymatic degradation of regular network aliphatic polyesters, React Funct Polym 1996;30(1):165-171. doi:10.1016/1381-5148(95)00107-7

FIGURE CAPTIONS

Figure 1. Synthesis scheme for the different studied copolyesters.

Figure 2. FTIR spectrum of PBSeT-70 sample. The inset compares the methylene bands of the three copolymers when spectra were normalized with the intensity of the C=O band.

Figure 3. ^{1}H NMR spectrum of PBSeT-70 . The inset shows a magnification of the 4.70-4.25 ppm region where the OCH_2 sequence sensitive signals appear.

Figure 4. DSC traces corresponding to the first heating run of PBSeT-30 (a), PBSeT-50 (b) and PBSeT-70 (c) as-synthesized samples. The cooling run from the melt state of PBSeT-70 (d) and the subsequent heating run (e) are also given to show the three run protocol followed to characterize the samples as summarized in Table 3.

Figure 5. Storage modulus (*E*') and loss tangent curves of PBSeT-30 (solid lines), PBSeT-50 (dotted lines) and PBSeT-70 (dashed lines) copolyesters. Inset shows the small peak around 60 ºC that was observed in the loss tangent curve of PBSeT-30.

Figure 6. TGA and DTGA curves comparing the thermal degradation of the three PBSeT-30 (black lines), PBSeT-50 (blue lines) and PBSeT-70 (red lines) copolyesters.

Figure 7. Contact angle measurements for water (a) and fetal bovine serum (FBS) (b) onto films of PBSeT-30, PBSeT-50 and PBSeT-70. In the chart-box, the boxes represent the percentile 25%-75%, the bars represent the range 5%-95%, (x) indicate1% and 99% of the distribution, and (+) indicate the maximum and minimal values of the data. Tukey test, $p<0.05$ vs. PBSeT-30 (†), and vs PBSeT-70 (‡).

Figure 8. SEM micrographs showing epitelial-like MDCK cells adhered on films of PBSeT-30 (a), PBSeT-50 (b) and PBSeT-70 (c); arrows and asterisks point out the formation of

filopodia and the film surface, respectively. Adhesion and proliferation onto the indicated material of: d) COS-7 (fibroblast-like cells) and e) MDCK (epithelial-like cells). Data concerning the culture plate as positive control are also provided.

Figure 9. Plot of the variation of the remaining weight percentage during exposure time to pH 7.4 buffer at 37 ºC (a) and 70 ºC (b) hydrolytic medium for PBSeT-30 (violet squares), PBSeT-50 (orange circles) and PBSeT-70 (pink triangles). c) ^{1}H NMR spectrum (5.1-3.9 ppm region) of a PBSeT-30, PBSeT-50 and PBSeT-70 samples before and after exposure for 60 and 300 days to the hydrolytic medium at 70 ºC.

Figure 10. WAXD of PBSeT-30 and PBSeT-70 copolymers before and during hydrolytic degradation at 70 ºC (q is the scattering vector $2\pi/d$)

Figure 11. a) Plot of the variation of M_n / M_o the weight (■,●,▲) and number (□,○,Δ) average molecular weight of PBSeT-30 (■), PBSeT-50 (♦), and PBSeT-70 (▲) during exposure time to the hydrolytic medium at 70 ºC. Simulated degradation curves of PBSeT-70, PBSeT-50 and PBSeT-30 assuming a first order mechanism are plotted by pink, blue and brown solid a lines, respectively. Color dashed lines point out the change of degradation mechanism when the minimum molecular size of insoluble fragments is achieved (pink, blue and brown r for PBSeT-30, PBSeT-50 and PBSeT-70, respectively).

Figure 12. SEM micrographs showing the surface of the different PBSeT-X samples before and after 60 days of exposure to a pH 7.4 hydrolytic medium at 70 ºC and to a lipase from porcine enzymatic medium.

Figure 13. Enzymatic degradation of copolymers using lipase from porcine pancreas (a), lipase from *Pseudomonas cepacia* (b). WAXD profiles after degradation with lipase from *P. cepacia* (c).

Table 1. GPC molecular weight data and polymerization yields.

Copolymer	Yield (%)	M_n (g/mol)	M_w (g/mol)	PDI
PBSeT-30	91%	7,000	17,100	2.44
PBSeT-50	89%	6,700	17,400	2.59
PBSeT-70	90%	8,600	19,300	2.24

Table 2. Composition and sequence-distribution analysis of synthesized copolyesters.

Copolymer	Composition Molar Fraction		Fraction of Diads Centered in the Butylene Units				Probability of Finding Units		Block Lengths		Degree of Randomness
	f_{Se}	f_T	f_{TT}	f_{TSe}	f_{SeT}	f_{SeSe}	P_{TSe}	P_{SeT}	L_{nT}	L_{nSe}	r
PBSeT-30	0.35	0.65	0.45	0.23	0.23	0.10	0.34	0.70	2.94	1.43	1.04
PBSeT-50	0.55	0.45	0.19	0.25	0.25	0.31	0.57	0.45	1.75	2.22	1.02
PBSeT-70	0.69	0.31	0.13	0.22	0.22	0.43	0.63	0.34	1.59	2.94	0.97

Table 3. Calorimetric data for the studied copolyesters.

Sample	1st Heating Run			Cooling Run			2nd Heating Run		
	T_m (ºC)	ΔH_f (J/g)	χ^a	T_c (ºC)	ΔH_c (J/g)	T_g (ºC)	T_m (ºC)	ΔH_f (J/g)	χ^a
PBSeT-30	163	-, 34	-, 0.38, (0.24)	-, 132	-, 35	-28	163	-, 38	-, 0.43, (0.26)
PBSeT-50	42, 106	9, 8	0.07, 0.13, (0.10)	11, 9	12, 9	-34	36, 112	12, 9	0.09, 0.15, (0.12)
PBSeT-70	47, 89	38, 2	0.25, 0.05, (0.19)	24, -	34, -	-39	45, 89	39, 3	0.25, 0.08, (0.21)

[a] Degree of crystallinity estimated for each phase considering the melting enthalpy reported for a 100% crystalline PBT sample (i.e. 142 J/g),[19] the estimated value for 100% crystalline PBSe sample (210.8 J/g)[20] and the experimental composition determined by ^{1}H NMR (i.e. $\chi_T = \Delta H_T / (\Delta H_T^{100} \times m_T)$ and $\chi_{Se} = \Delta H_{Se} / (\Delta H_{Se}^{100} \times m_{Se})$, being m_T and m_{Se} the mass fraction of each repeat unit). The total crystallinity ($\chi = \Delta H_{Se} / (\Delta H_{Se}^{100}) + \Delta H_T / (\Delta H_T^{100})$) is given in brackets.

Table 4. DMTA data of the studied copolyesters.[a]

Sample	T_g (ºC)	$E'_{-40\,ºC}$ (MPa)	$E'_{-20\,ºC}$ (MPa)	E'_{20} (MPa)
PBSeT-30	-5.3	2357	2040	406
PBSeT-50	-11.7	2040	1183	171
PBSeT-70	-14.3	1478	924	265

[a] Storage moduli are given for temperatures before (-40 ºC) and after (-20 ºC) the first glass transition temperature and after the second glass transition temperature (20 ºC).

Table 5. TGA and DTGA data for thermal decomposition of the studied copolyesters.

Sample	T_{onset} (ºC)	$T_{1st\ step}$ (ºC)	$T_{2nd\ step}$ (ºC)	$W_{1st\ step}$ (%)	*Char yield (%)*
PBSeT-30	322	405	456	3	5.2
PBSeT-50	337	406	456	6	2.6
PBSeT-70	356	409	453	8	3.3

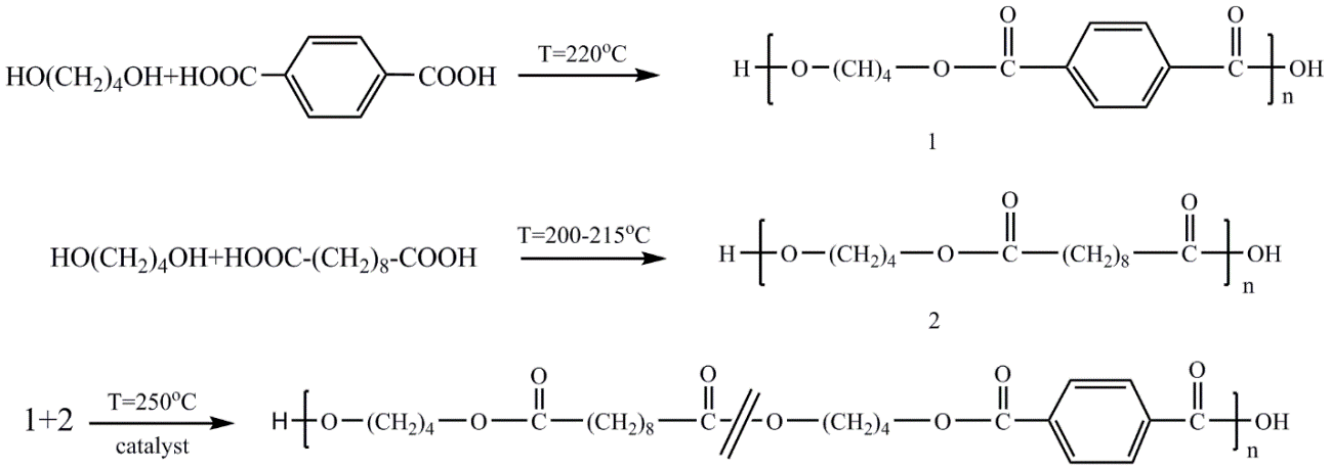

Figure 1

Heidarzadeh *et al.*

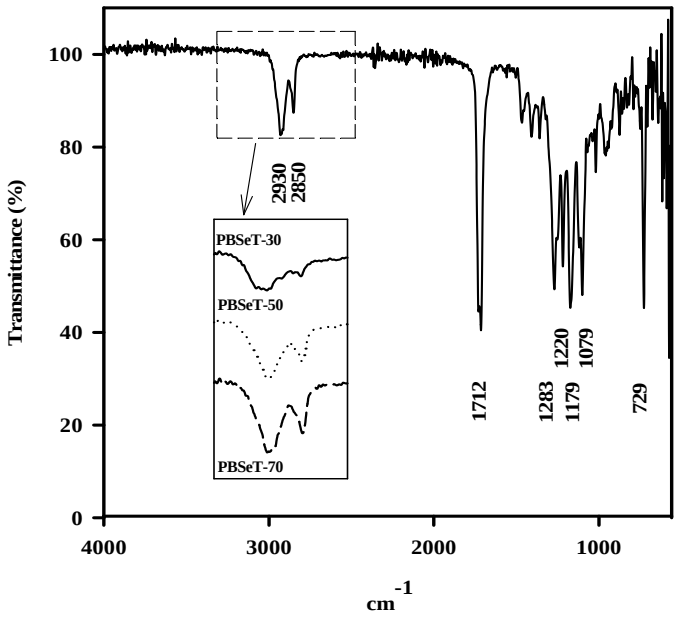

Figure 2

Heidarzadeh *et al.*

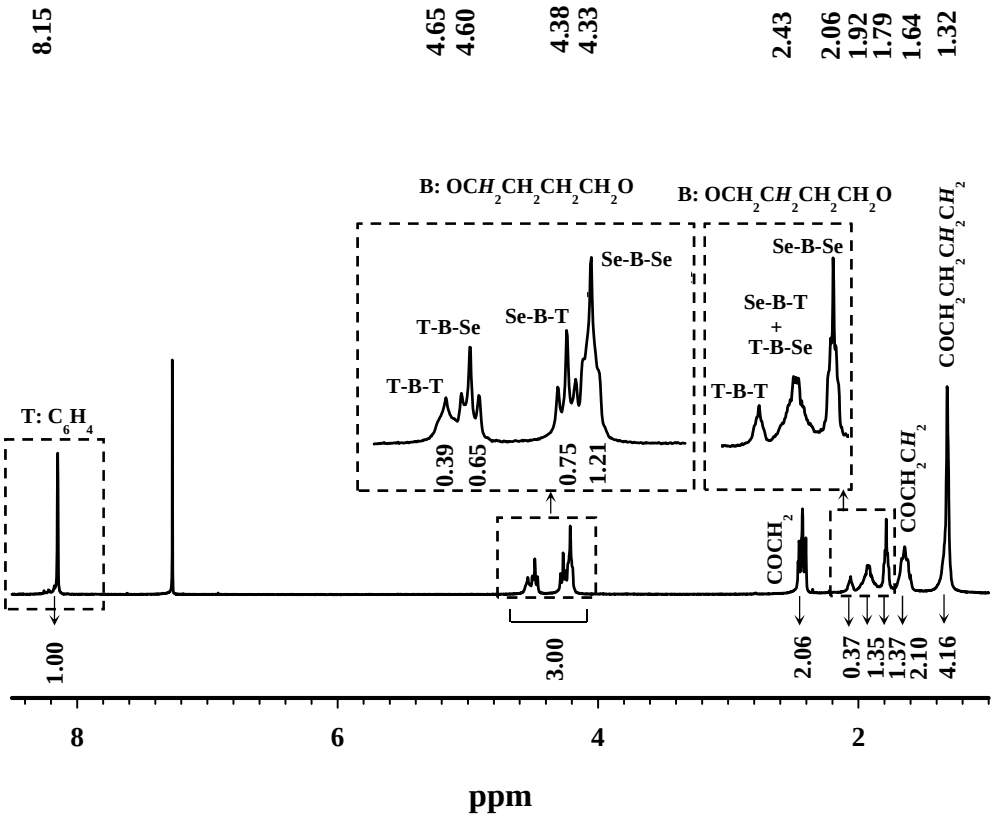

Figure 3

Heidarzadeh *et al.*

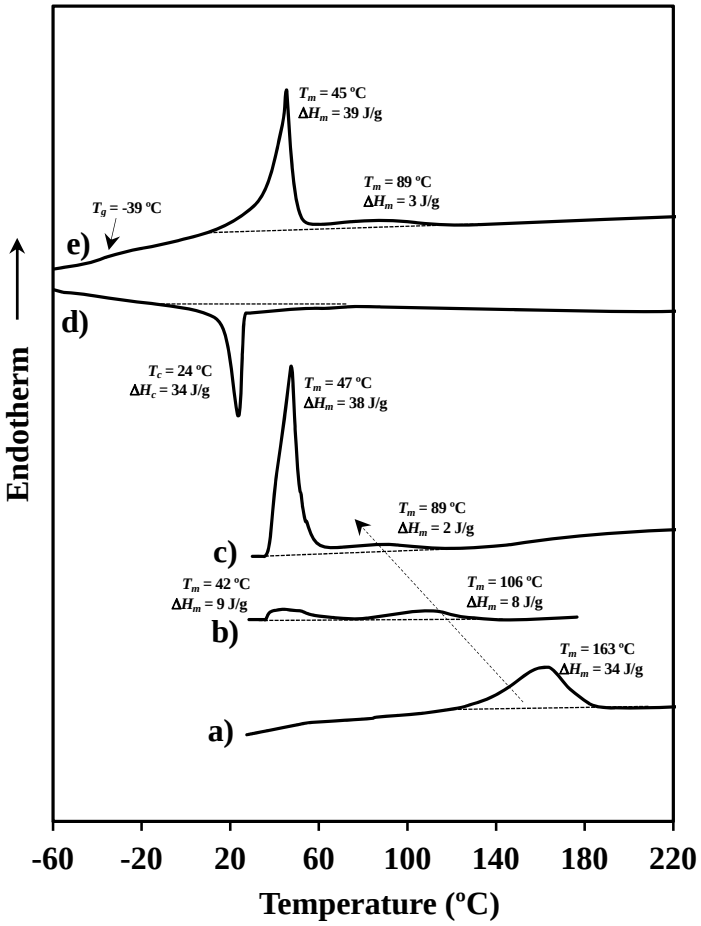

Figure 4

Heidarzadeh *et al.*

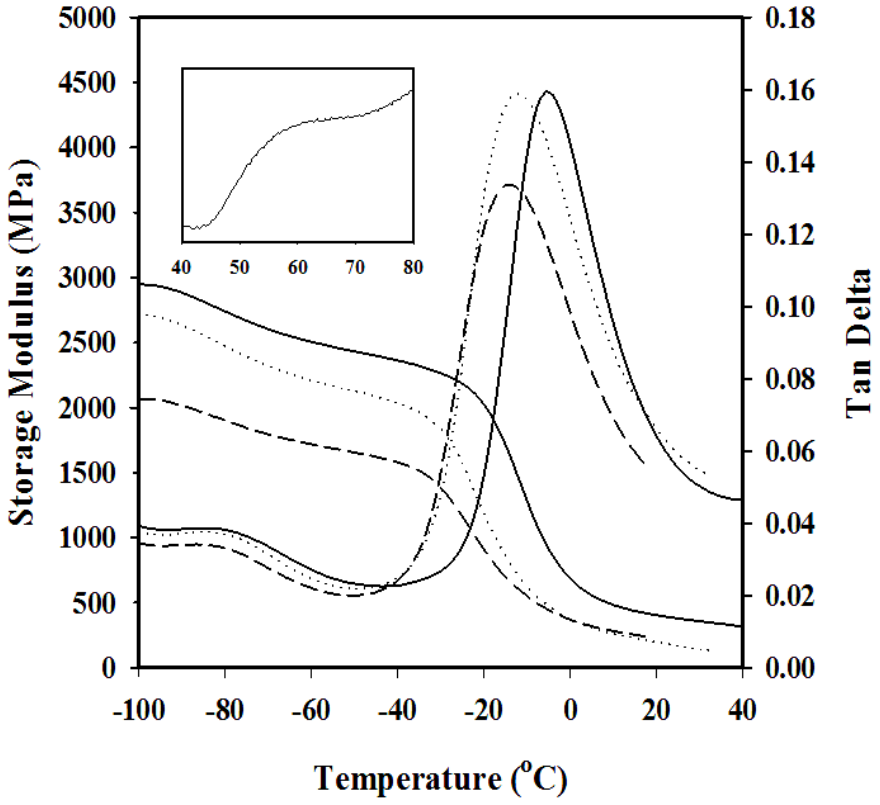

Figure 5
Heidarzadeh *et al.*

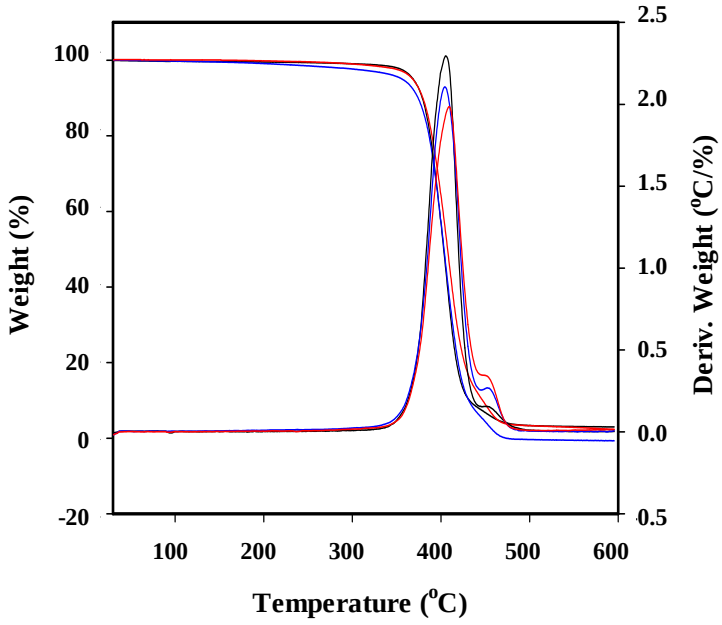

Figure 6

Heidarzadeh *et al.*

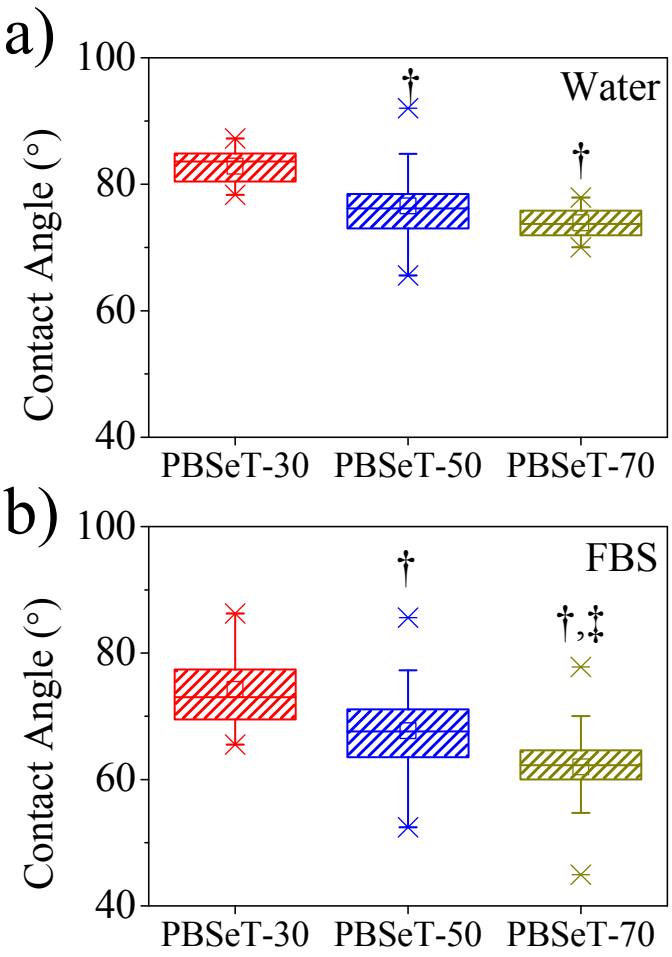

Figure 7
Heidarzadeh *et al.*

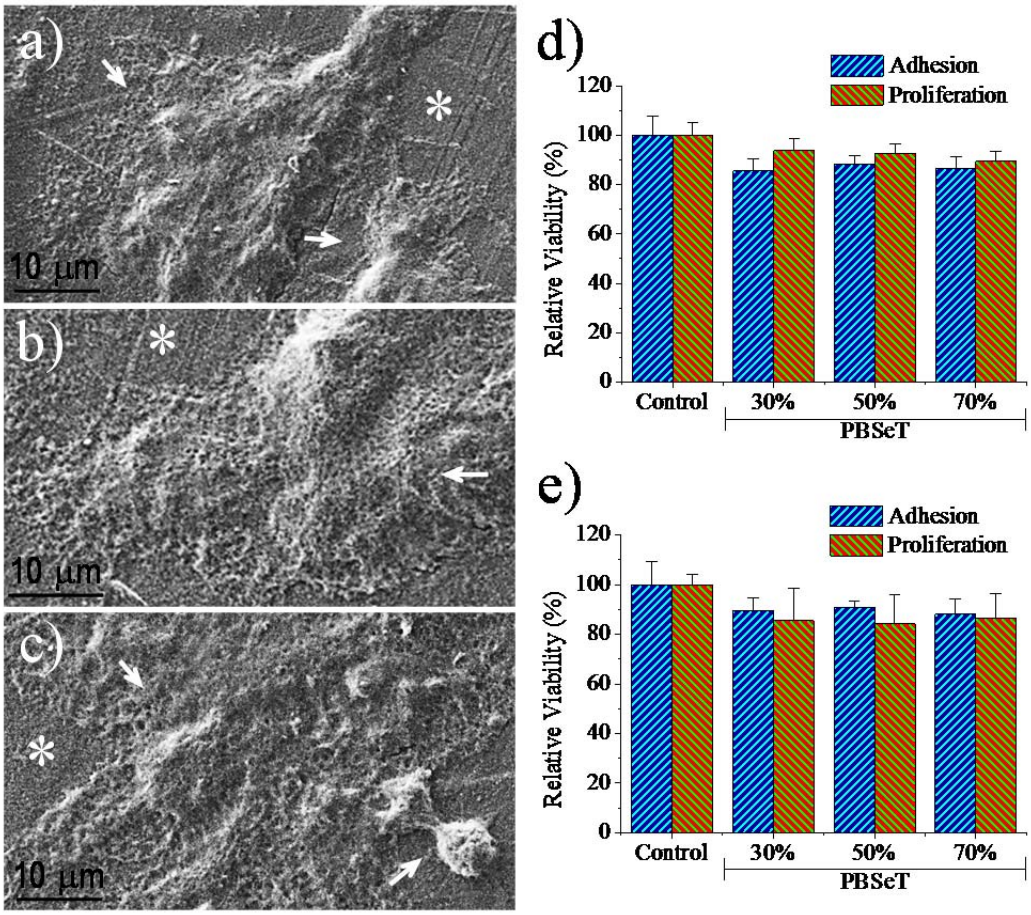

Figure 8

Heidarzadeh *et al.*

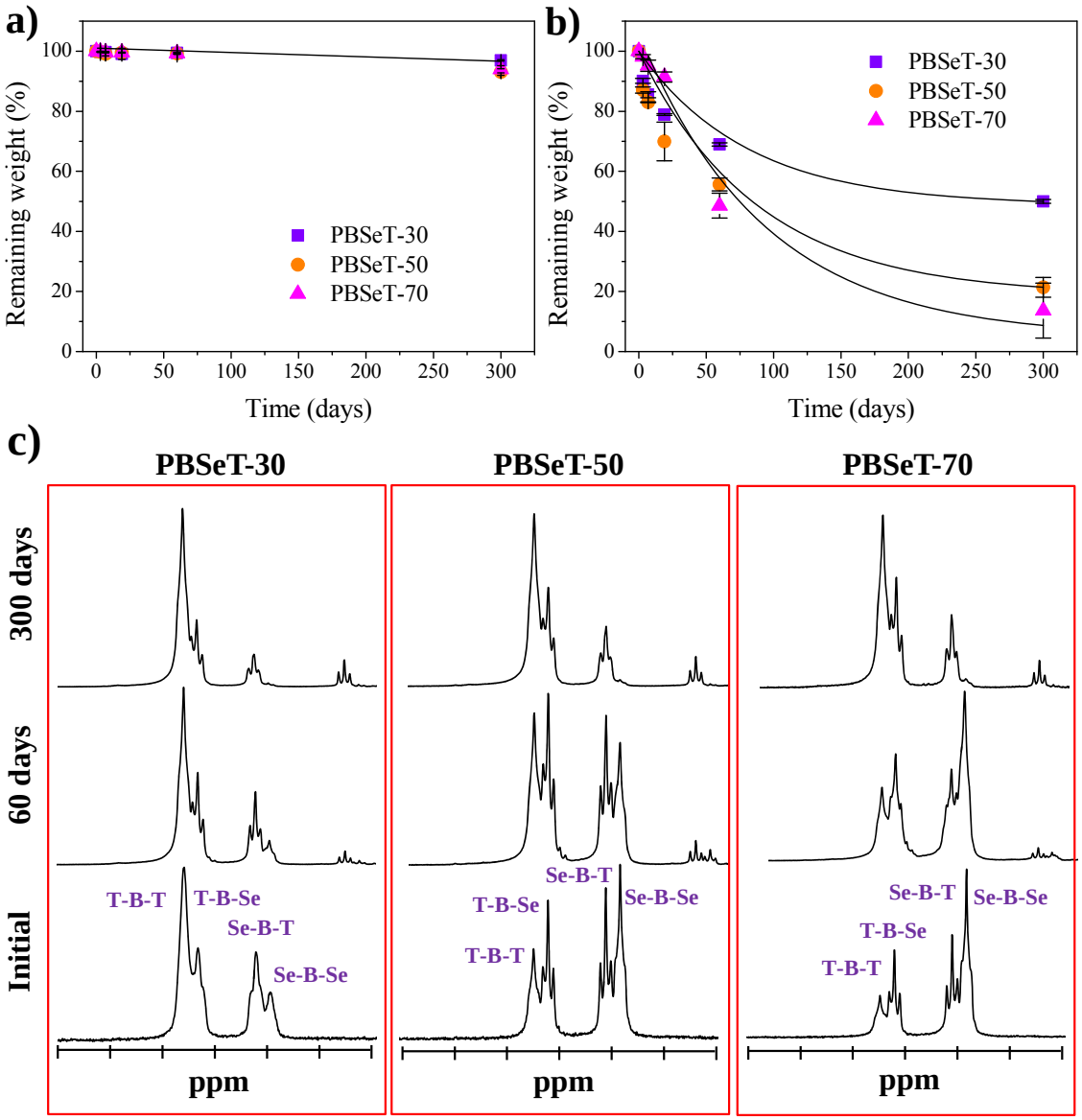

Figure 9

Heidarzadeh *et al.*

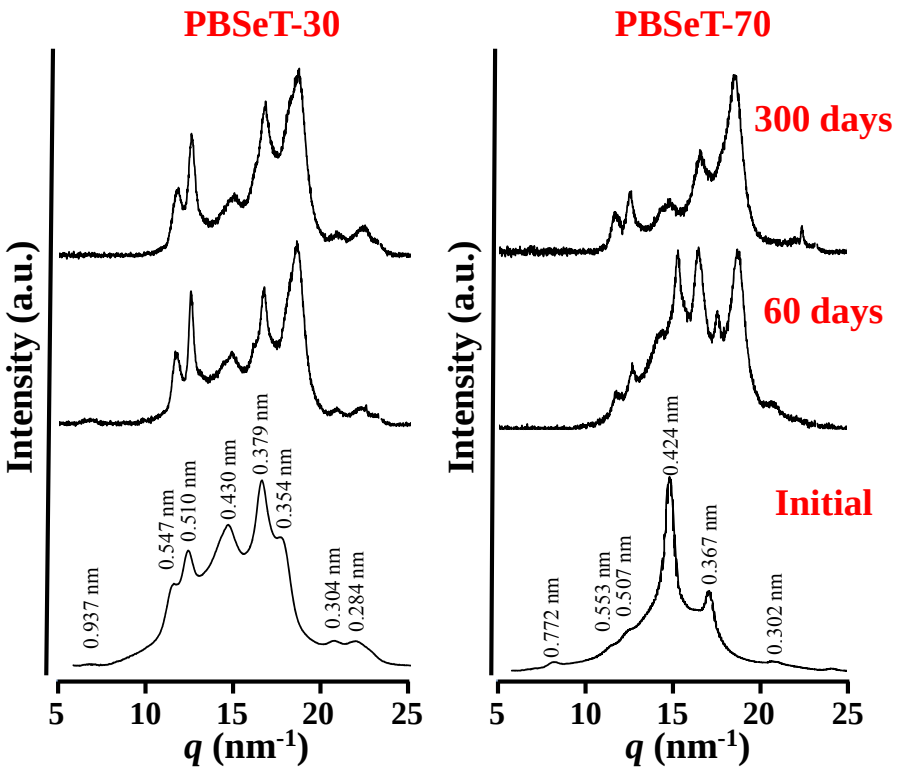

Figure 10

Heidarzadeh *et al*.

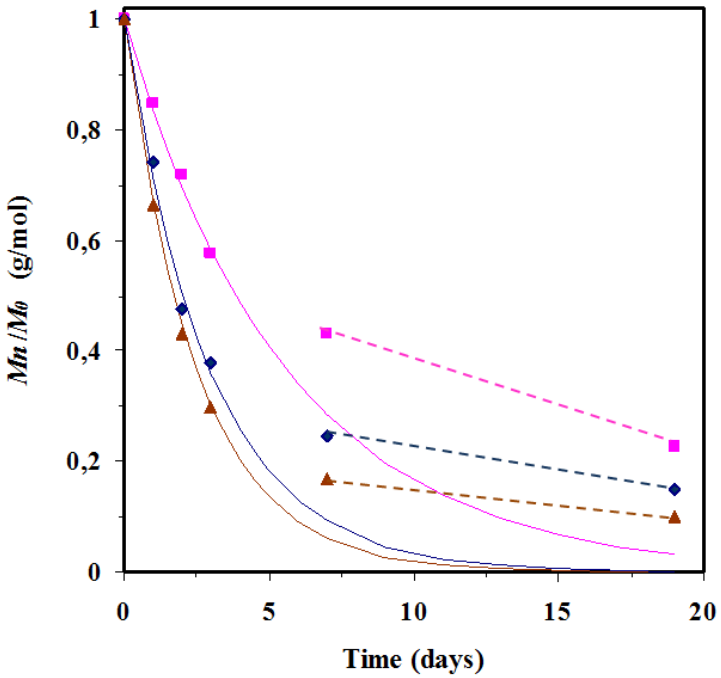

Figure 11

Heidarzadeh *et al.*

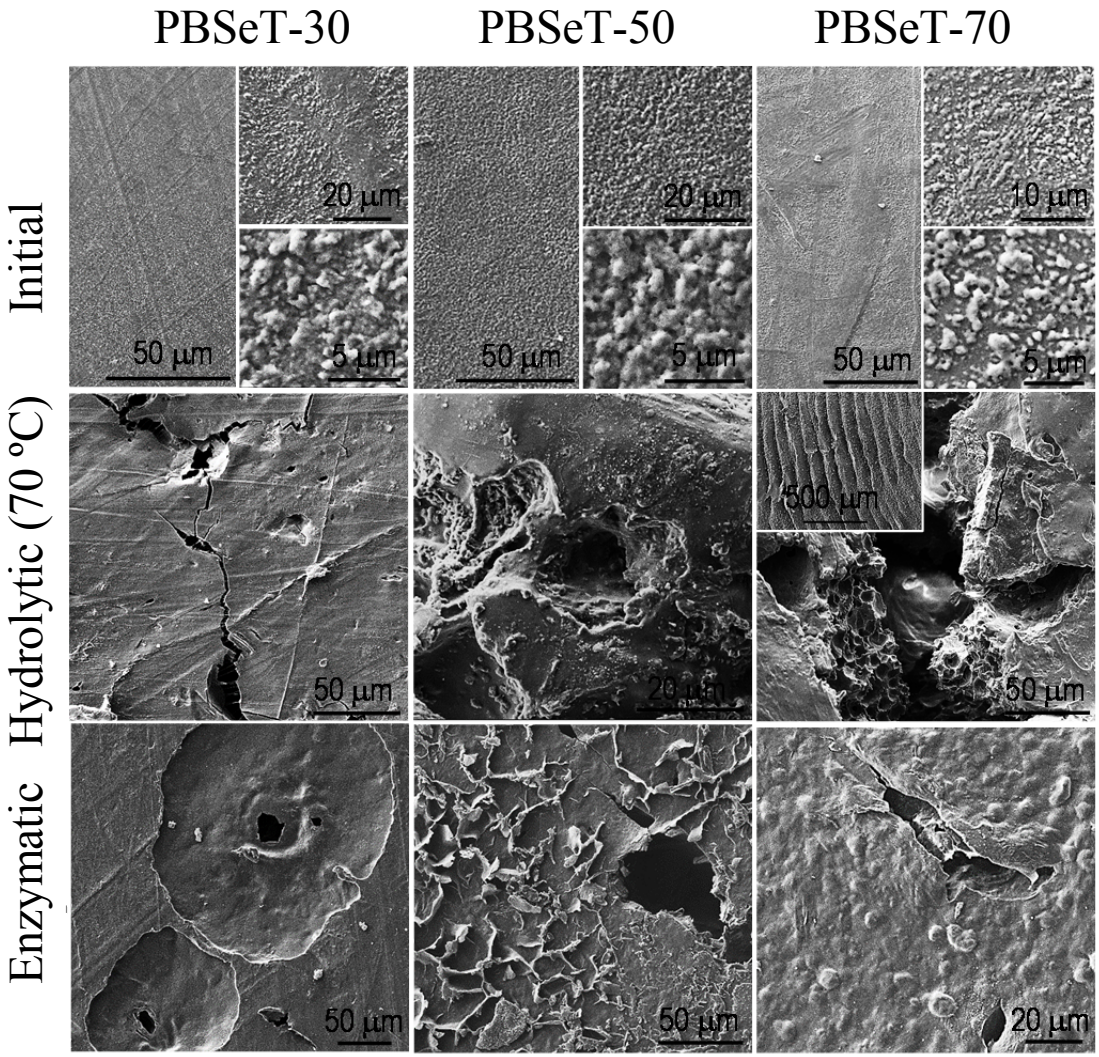

Figure 12

Heidarzadeh *et al.*

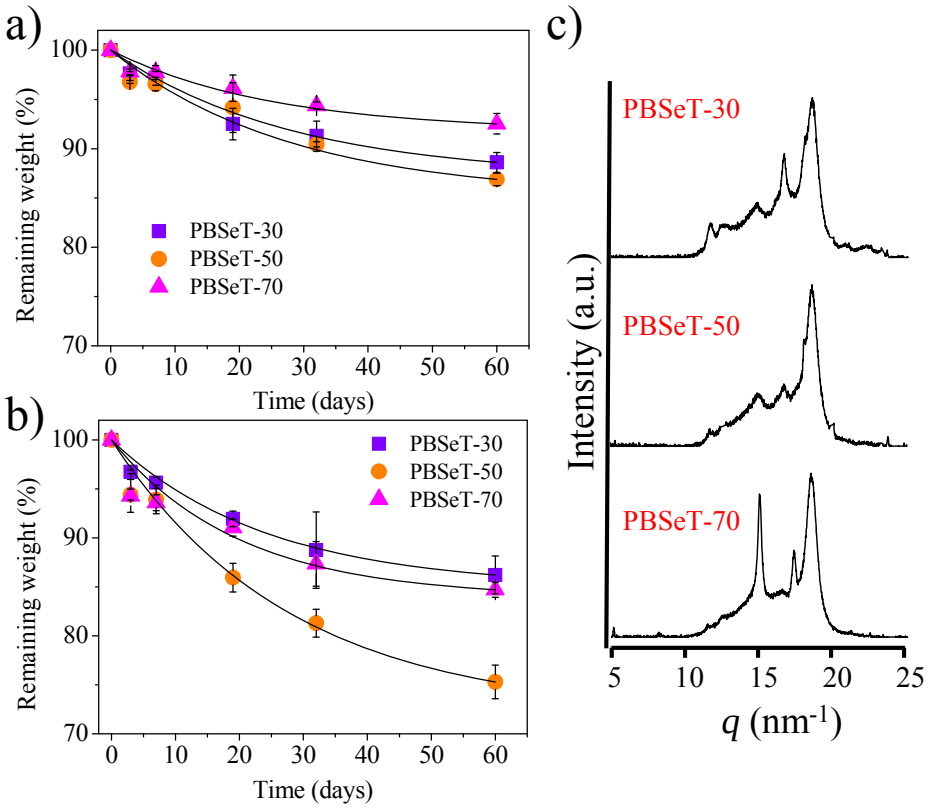

Figure 13

Heidarzadeh *et al.*